Astron. Astrophys. 331, 231–243 (1998)

ASTRONOMY AND ASTROPHYSICS

Period variation and surface activity of the contact binary VW Cephei

G. Kaszás[1], J. Vinkó[1], K. Szatmáry[2], T. Hegedüs[3], J. Gál[2], L.L. Kiss[2], and T. Borkovits[3]

[1] Department of Optics, JATE University, P.O. Box 406, Szeged, H-6701 Hungary
[2] Department of Experimental Physics, JATE University, Dóm tér 9., Szeged, H-6720 Hungary
[3] Baja Astronomical Observatory, P.O. Box 766, Baja, H-6500 Hungary

Received 28 August 1997 / Accepted 13 November 1997

Abstract. Long-term behavior of the well-known contact binary VW Cephei is discussed based on new multicolor (BV) photometry made over 8 years and high-resolution spectroscopy. The existence of an at least 7 year-long activity cycle is confirmed using light curve disturbances as the indicator of surface brightness variations. The orbital period of the system has been decreased further in accordance with previous predictions. It is shown that the cyclic component of the period variation ($O-C$) curve has an amplitude too large to be fully due to the light-time effect of the astrometric 3rd companion. It is suspected that the magnetic activity cycle of the primary component affects the orbital period significantly. Simultaneous solution of light- and velocity curves (obtained during the "quiet" stage) resulted in new parameters of the system. The mass ratio (q = 0.35) is considerably larger than the previous spectroscopic value given by Hill (1989). High resolution optical spectroscopy made at the beginning of the new active cycle reveals $H\alpha$ emission arising from the chromosphere of the primary whereas the secondary lacks such emission. This fact gives further support to the theoretical prediction that the primary component drives the activity of contact binaries. Fitting cool spots (ΔT_{eff} = 2000 K) to the surface of the primary, the minimum spot coverage was found to be 12 % at the active stage, while it is about $1-2$ % at the quiet stage. An anticorrelation of $H\alpha$ emission and spot position has been pointed out.

Key words: stars: individual: VW Cep – binaries: eclipsing – stars: activity – stars: variables

1. Introduction

VW Cephei (HD 197433 = BD +75 752 = SAO 9828) is one of the best observed variable stars. This star is a well-known, representative member of its class, the W UMa-type eclipsing binaries. These variables have some special observable properties which make them relatively easy to classify based on their light variation. Basically, W UMa-stars are eclipsing binaries of two components having later spectral type (usually between F and K), nearly equal surface brightnesses (and probably similar surface temperatures) but very unequal mass (the mass ratio can be $q < 0.1$ in some cases and its average value is less than 0.5 for the known variables). The light variation is continuous along the orbital cycle, so the beginning and end of eclipses are undistinguishable from the uneclipsed light variation (the latter is due to the distortion of the components). Due to the nearly equal surface brightnesses, the eclipses have comparable depth (the difference between eclipse depths is usually less than 20 percent of that of the primary eclipse), and the color variation is usually small – e.g. the observed change in $B-V$ can usually be entirely attributed to the effect of gravity darkening.

The observed light variation of W UMa-type variables were successfully explained by the contact model introduced by Lucy (1968). Assuming that both components fill their Roche-lobe the light variation can be modeled successfully, although detached configurations with very distorted components give almost equally good fit to the light curve shape. It is worth mentioning that, due to this ambiguity, the shape of the light curve alone does not justify the need of the contact model. It is the temperature equalization provided by the observed constancy of the color (and perhaps some other spectroscopic evidence) that makes the contact configuration necessary – without being in actual contact the components having very unequal mass cannot have the same surface temperatures.

Although Kuiper (1941) argued that radiative stars with unequal mass on the ZAMS cannot be stable in a contact configuration, Lucy (1968) showed that systems embedded in a common convective envelope can remain in actual contact on the main sequence. For the time being, the Lucy-model is the most widely accepted model of the W UMa-type contact binaries. The so-called early type contact systems have similar observational characteristics, but these are in contrast with the

Send offprint requests to: kaszas@physx.u-szeged.hu

convective envelope hypothesis. In this point of view the early type systems are still misterious, but these are not considered in this study.

The Lucy model predicts that the more massive component must always have slightly higher temperature (thus it has larger surface brightness) than the less massive secondary, indicating that the primary eclipse should be due to transit (i.e. the smaller, less massive star is in front). However, comparing the light curves with radial velocities derived from spectroscopic observations, it is revealed that the majority of W UMa-stars show occultation eclipses during primary minimum (the more massive star receeds after primary minimum indicating that it was in front during the eclipse). This phenomenon was the basis of the classification proposed by Binnendijk (1970) who divided the W UMa-stars into two groups: A-type with primary eclipse as transit and W-type with primary eclipse as occultation. The phenomenological explanation of this A/W dichotomy was presented by Rucinski (1974) introducing the concept of hot secondary (HS). In this model the secondary has a temperature excess $X = (T_{sec} - T_{pri})/T_{pri}$ for a physically unknown reason. Although this model turned out to be inadequate for explaining the measurements made in the far ultraviolet (Eaton et al. 1980), this hypothesis has been widely accepted among observers in the modeling of the measured light curves with a computer synthesis code (e.g. the Wilson-Devinney [*WD*] code, Wilson & Devinney, 1971; Wilson, 1979).

An alternative explanation of the A/W dichotomy was proposed firstly by Mullan (1975) introducing starspots on the surface of the primary component. This model was also favoured by Eaton et al. (1980) showing that the observations can be modeled by starspots distributed equally along the equator of the primary. The newer versions of the *WD* code incorporate the ability of spotfitting, thus, it is possible to fit the geometric parameters and the spot coordinates simultaneously. In practical applications, however, this must be done carefully, because too many free parameters may render the solution indeterminate. A more sophisticated approach based on Maximum Entropy Method was presented recently by Hendry et al. (1992) for VW Cephei itself. The spot model can most successfully explain the changing asymmetries of the light curve (unequal maxima, minima with varying and/or alternating depth).

The light variation of VW Cephei was discovered by Schilt (1926). The apparent average magnitude of this system is V = 7.5 mag, so VW Cep is one of the brightest member of its class, which makes it relatively easy to observe. The orbital period is short, P = 0.27831 day, therefore it is possible to observe the whole orbital cycle during one night. These circumstances explain the popularity of VW Cep among observers, as indicated e.g. by the number of papers attributed to the study of VW Cep in $IBVS$.

Fortunately, VW Cep is worth observing continuously, because the system produces a lot of phenomena that are characteristics of W UMa-type eclipsing binaries. It shows a) O'Connell-effect having unequal maxima, b) increased surface activity changing the shape of the light curve and the depth of eclipses and c) light-time effect due to a third companion that was discovered astrometrically by Hershey (1975). The first international campaign for multi-site photometric observations was organized by Kwee (1966a,b). The main result of that study was the discovery of the light curve changes. After that, a lot of light curves in different wavelength bands were published by many authors almost every year, which made VW Cep one of the best observed variable stars.

Many alternative models were published to explain the disturbances of the light curve including circumstellar ring (Kwee, 1966c), precession of rotational axes (Walter, 1979), hot spot due to gas stream (van't Veer, 1973; Pustylnik & Sorgsepp, 1976), dark starspots (Yamasaki, 1982; Linnell, 1986, 1991; Hendry et al., 1992). The latter model turned out to be the most realistic one. The possibility of dark starspots on the surface is supported by some other phenomena observed in the VW Cep system that are usually considered as indicators of enhanced stellar surface activity. These are: *i.)* increased $H\alpha$ emission, probably emitted by the chromosphere (Barden, 1985); *ii.)* fast rotation velocity, i.e. large Rossby-number (Vilhu & Walter, 1987; Rucinski, 1993); *iii.)* flare events observed in many bandpasses from radio to X-ray (Vilhu et al., 1988); *iv.)* slow cyclic change of the frequency and strength of light curve disturbances similarly to the sunspot cycle (Bradstreet & Guinan, 1988). The correct physical mechanism of the assumed activity is still not clear, the sun-like dynamo driven by stellar magnetic field is the most likely explanation. Recent computations provided by Stepien (1995) suggest that magnetic fields play important role in the formation of contact binaries via magnetic braking. In addition, the hard X-ray flux observed by *Ginga* indicates coronal temperature of the order of 10 keV. This very high temperature is thought to be due to some kind of magnetic effect in the binary system (Tsuru et al., 1992). However, the lack of detection of VW Cep in 2, 6 and 20 cm wavelength bands (Rucinski & Seaquist, 1988) indicates that the system is rather inactive in the radio domain, contrary to the expectations based on the strong activity in other spectral regions.

The spectroscopic observations of VW Cep are much less numerous compared with the photometric ones. This is probably due to the short orbital period of the system and the highly broadened, complicated spectral lines that require large telescopes in order to reach sufficient signal-to-noise ratio. The first spectroscopic observation was made by Popper (1948) who determined a combined spectral type of $G8 - K0$ and gave the mass ratio as q = 0.33. Later, Binnendijk (1967) derived q = 0.41 from his spectra. Recently high- and medium-resolution spectroscopic observations were published by Hill (1989) and Frasca et al. (1996). Hill (1989) derived a spectroscopic mass ratio, q = 0.27, that was significantly lower than the previous results. He used the sophisticated cross-correlation technique that makes the results more realistic than the previous solutions. The disagreement is mainly due to the complicated line profiles mentioned above, that are difficult to measure with a low dispersion spectrograph and photographic detector which were often used in the past. In the case of VW Cep, an additional complication is caused by the light of the third component. Because its lines are much less broadened than those of the eclipsing pair, these lines

disturb the line profile of the contact binary significantly, in spite of the fact that the light of the third companion represents only less than 10 percent of the total intensity of the system in the optical band.

2. Observations

2.1. Photometry

Our photometric monitoring of VW Cep was begun in 1987 at Baja Observatory, Hungary with the 40 cm Cassegrain-type telescope of JATE University. In 1991 the instrument was moved to the newly opened Szeged Observatory. After that, the 50 cm Cassegrain-type telescope of Konkoly Observatory, installed at Piszkéstető mountain, was also used frequently for studying VW Cep. The measurements were made through Johnson V and B filters with both telescopes. The transformation coefficients of the instruments were calibrated every year in order to ensure maximal accuracy in the standard transformation.

The differential photometric observations were obtained using two comparison stars in the vicinity of VW Cep. In the 1987-88 season the light variation of VW Cep was measured with respect to HD 200251. This star was used as a comparison by several earlier observers, although it is listed in the "New Catalogue of Suspected Variable Stars" (NSV 13442). We could not point out any significant variation in its brightness during our observing runs. Later, HD 199476 was chosen as comparison star, because it is closer to the variable than HD 200251. All the previous magnitudes that were obtained with respect to HD 200251, were transformed into differential magnitudes with respect to HD 199476. Because differential magnitudes are sufficient for light curve analysis, calibration to absolute photometry was not performed.

In Fig. 1 we present seasonal light curves of VW Cep in order to illustrate the variations of the shape of the light curve. Note that $\phi = 0.0$ was assigned to the $transit$ minimum (smaller, less massive star is in front) and not the primary minimum which is due to occultation (since VW Cep is a W-type contact binary). Some of the seasonal light curves were already published in earlier papers (Vinkó, 1989; Vinkó et al., 1993; Kiss et al., 1995) together with their ephemerides. The data obtained in 1995 were folded with the following ephemeris:

$$HJD_{min} = 2449907.4267 + 0\overset{\mathrm{d}}{.}2783083\ E.$$

The extensive list of individual measurements are available upon request via e-mail.

It is known that VW Cep can show O'Connell-effect as large as 0.1 mag during activity maximum. The light curve variations observed during this project fully confirm the results of previous studies. These are: i) changing, unequal heights of maxima and depths of minima and ii) varying out-of-eclipse mean magnitude. Both of these can be most easily seen comparing the V light curves of the 1992 and 1995 seasons. Our observations indicate that the system showed less and less activity between 1988 and 1993, then the light curve perturbations became strong again in 1995. According to earlier observations, the system was in activity maximum in 1986-87, thus, the new observations presented here confirm the cycle-length of the activity variation of VW Cep (about $7-8$ years) proposed by Bradstreet & Guinan (1988). In addition, we detected some night-to-night changes of the light curve in August-September 1992 when the system was observed most frequently, but these were very close to the noise level ($0.01-0.02$ mag), thus, the precision of our data was not good enough to study these slight variations further, except to note that a similar phenomenon was reported earlier by Kreiner & Winiarski (1981).

The seasonal light curves were used for determining the geometric parameters of the system as described in Sect. 3. The multi-year observations allowed us to separate the changes due to eclipses and geometric distortions and the light curve perturbations which we further assume to be due to dark starspots. Therefore, the 1992 seasonal light curve was studied to solve for the parameters of the system, and the data from 1995 was used for spotfitting.

2.2. Spectroscopy

The spectroscopic measurements were obtained on 18/19 September, 1995 at David Dunlap Observatory (Richmond Hill, Canada) using the Cassegrain spectrograph attached to the 74" telescope. The spectra were centered at 6600 Å with a reciprocal dispersion about 10 Å/mm giving a resolving power $\lambda/\Delta\lambda \approx 11,000$. The detector was a Thomson 1024×1024 CCD with readout noise about 5 e^-. The spectra were reduced with standard $IRAF$ routines including bias correction, flat fielding and cosmic ray removal. For wavelength calibration, two FeAr spectral lamp exposures were obtained after every fourth stellar exposure. The integration time was set to 8 minutes which corresponds to $\Delta\phi \approx 0.02$ phase variation, in order to avoid the smearing of the line profiles due to the orbital revolution. The signal-to-noise was usually between 50 and 100. 40 such spectra covering the whole orbital cycle were obtained (all of them are available from the authors upon request).

The width of the recorded spectral interval was 200 Å, containing the $H\alpha$ line and several weak photospheric (mostly FeI) lines. For calibrating the velocity system, two IAU velocity standard stars (HD 204867, Sp=$G0$ and HD 212943, Sp=$K0$) were also measured before VW Cep and reduced in the same way. Telluric lines were absent in the $6600-6700$ Å spectral regime, but affected heavily the $6500-6550$ Å region, the blue side of $H\alpha$.

The telluric lines were eliminated from the spectra using an iterative method. The telluric correction is not a trivial problem, because the depth of telluric lines change quite considerably depending on the airmass of the object and the humidity of the atmosphere. Moreover, this procedure needs correct identification of as many telluric lines as possible. This latter problem was solved observing a rapidly rotating $A0V$-type star (HD 177724) as a telluric standard. As a possible solution of the former problem, the telluric standard was observed on the same night as VW Cep through similar airmass.

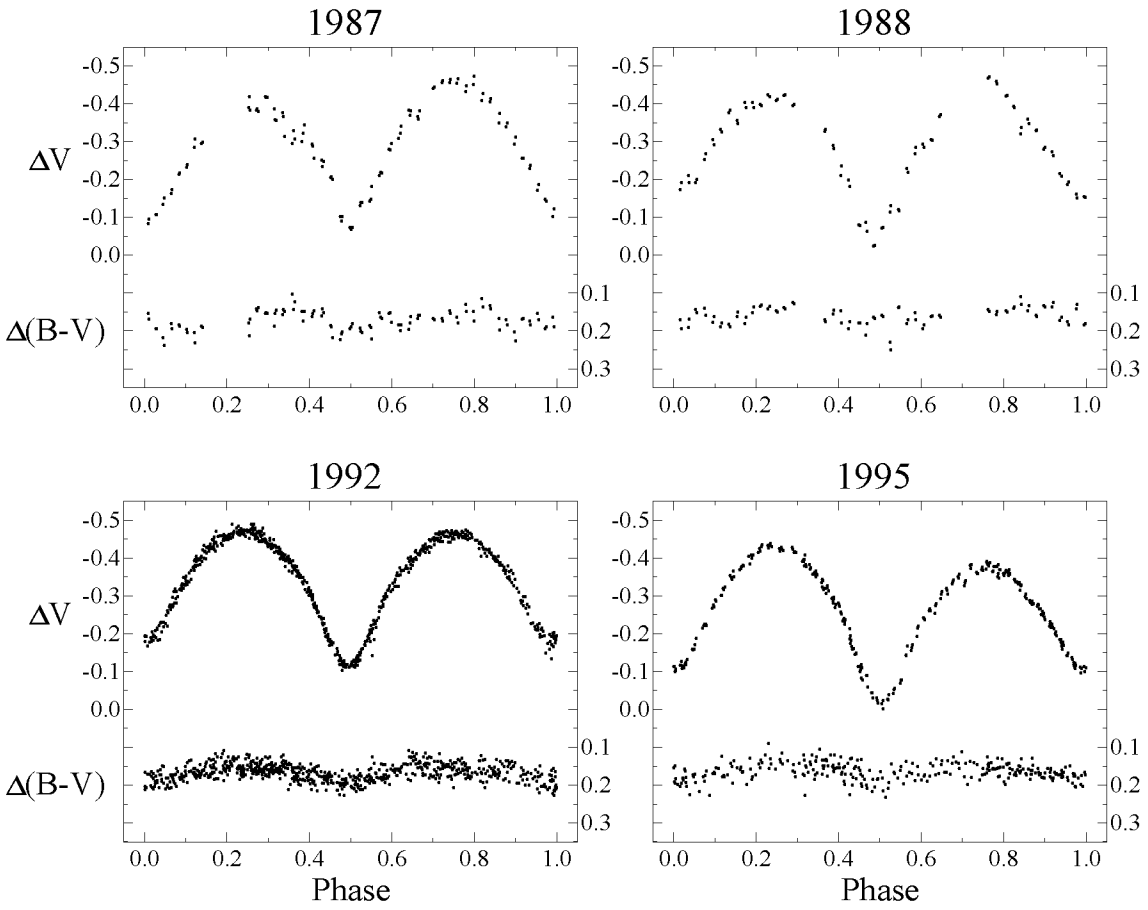

Fig. 1. V and $B-V$ light curves of VW Cep obtained in different seasons. The variation due to the different level of activity is apparent. The 1992 curve seems to be undisturbed, so this light curve was adopted as the "immaculate" or spotless curve for further analysis.

The pure telluric spectrum was constructed from the original telluric standard spectrum by subtracting the stellar contribution. The telluric-free spectrum of the standard star was determined iteratively using gaussian smoothing. The idea was that the fast-rotating, early-type star has a smooth, slowly varying spectrum, while the telluric lines are sharp features that could be removed by a smoothing process. However, the smoothing should not distort the strong $H\alpha$ line of the standard star, therefore the $FWHM$ of the smoothing gaussian was set to a lower value within $H\alpha$, while a stronger smoothing was allowed outside that region. The minimum value of $FWHM$ was 1 Å in the $H\alpha$ region and 15 Å outside that. Next, this smoothed stellar spectrum was subtracted from the original one in order to produce the pure telluric spectrum. After that, the telluric standard spectrum was divided by this pure telluric spectrum resulting in a better estimate of the stellar component. The whole cycle was then iterated until no improvement has been found in the pure telluric spectrum.

Note, that similar smoothing technique (with fixed $FWHM$ = 0.1 Å) was also used for the VW Cep and comparison star spectra in order to reduce the instrumental scattering. The change of the depth of spectral lines caused by this procedure was below 0.001 in intensity units.

Finally, the telluric lines from both the spectra of VW Cep and the comparison star were eliminated dividing each spectrum by the pure telluric spectrum. In order to reduce the artificial scattering, the division was done only for telluric lines having at least 0.01 line depth in intensity units.

In order to derive new radial velocity curve of VW Cep, the spectra were cross-correlated with both velocity standard stars using the $6600-6700$ Å wavelength regime (which is practically free of telluric lines). The cross-correlation function (ccf) was determined in the $[-500,500]$ km s^{-1} interval for every VW Cep spectrum. There were no significant differences between the ccfs obtained with the two different template stars (except the horizontal shift due to the different relative velocities). The velocity corrections due to the motion of the Earth were computed with the $IRAF$ task $rvcorrect$. Fig. 2 shows some sample ccf functions illustrating the quality of the data. The primary as well as the secondary exceeds the noise level, so the signal-to-noise ratio was high enough to detect the contact binary components. The third component can also be clearly seen as the narrow feature close to zero radial velocity.

As mentioned in the Introduction, the third component affects the line (as well as ccf-) profiles of VW Cep. This results in the disturbing fact that the maximum of the measured ccf does

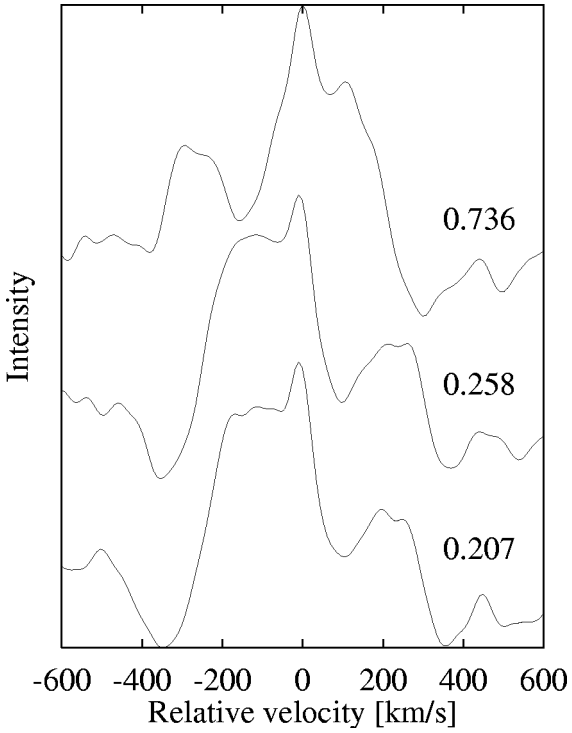

Fig. 2. Cross-correlation function (ccf) profiles of VW Cep at various orbital phases. Note the presence of the third component close to zero radial velocity.

Table 1. Heliocentric radial velocities of VW Cep (in km s^{-1}).

Hel.JD.	Phase	V_{rad}^{Pri}	V_{rad}^{Sec}
2449979.5695	0.2163	-101	189
2449979.5753	0.2371	-101	211
2449979.5811	0.2579	-121	229
2449979.5869	0.2786	-121	229
2449979.5961	0.3116	-116	219
2449979.6019	0.3324	-106	179
2449979.6077	0.3532	-86	164
2449979.6134	0.3740	-56	144
2449979.6865	0.6367	49	-181
2449979.6923	0.6575	29	-256
2449979.7025	0.6941	54	-279
2449979.7083	0.7149	59	-256
2449979.7141	0.7356	79	-271
2449979.7199	0.7564	74	-266
2449979.7268	0.7814	59	-266
2449979.7326	0.8022	49	-251
2449979.7384	0.8230	44	-241
2449979.7442	0.8438	39	-221
2449979.8143	0.0958	-91	154
2449979.8201	0.1165	-76	119
2449979.8280	0.1448	-96	144
2449979.8338	0.1656	-111	154
2449979.8395	0.1864	-106	194
2449979.8453	0.2072	-121	194

not necessarily coincide with the maximum of the ccf of the contact binary itself, therefore, assigning the velocity of the ccf maximum to the velocity of the primary component one would underestimate the velocity amplitude of the primary (since the third component shifts the maximum toward smaller velocities). In order to take this into account, the third light peak was removed manually from the ccf profiles interpolating by eye. This undoubtedly reduced the precision of the ccf profiles, however, the true velocities of the primary (i.e. the maximum of the ccf) could be measured more reliably than without eliminating the third component. Nevertheless, a more rigorous third light correction procedure should be applied to more precise high-resolution spectroscopic data to reduce the uncertainties further.

Table 1 lists the new derived heliocentric radial velocities of the primary and the secondary component, respectively. Again, ϕ = 0.0 refers to the transit minimum. The errors are simple estimates of the uncertainty of the hand-drawn fitted curve. This new radial velocity curve of the primary component has slightly larger amplitude than that provided by Hill (1989) which affects the results of the determination of the physical parameters. Further analysis of the light- as well as the velocity curves are presented in the following section.

3. Physical parameters

It is somewhat surprising that, although many parameter determinations of a lot of W UMa-stars can be found in the recent literature (which are mostly based on multi-color light curve solutions), there are not too many modern solutions (i.e. simultaneous fitting of light- and radial velocity curves) for VW Cephei, despite its popularity among observers. This is probably due to the frequent changes of the light curve discovered decades ago as mentioned in the Introduction. Our long-term photometric monitoring together with the new radial velocities enabled us to look for a consistent physical model of VW Cephei combining both photometric and spectroscopic data.

The B and V light curves obtained during the 1992 season as well as the new radial velocity data collected in Table 1 were used for determining the physical parameters of the system. The average effective temperature of the primary was fixed at T_1 = 5050 K based on the observed $B-V$ = 0.86 color of the system (Eggen, 1967; Hill, 1989). As it was shown in many papers discussing light curve solutions, this parameter should be kept fixed to reduce the correlation between different parameters. The fractional intensities of the third light was set to 0.07 and 0.04 in V and B, respectively (Hendry et al., 1992).

The physical model of the contact binary was built based on the *BINSYN* code mentioned by Vinkó et al. (1996). The hot secondary hypothesis was used similarly to many earlier investigators. Linnell (1986, 1991) showed that the hot-secondary model could better reproduce the observed colors of the system than the spot model. Recent extensive computations including line profile fitting performed by Hendry (1997) indicate that the primary component is always more spotted than the secondary and the spots are distributed uniformly in most cases.

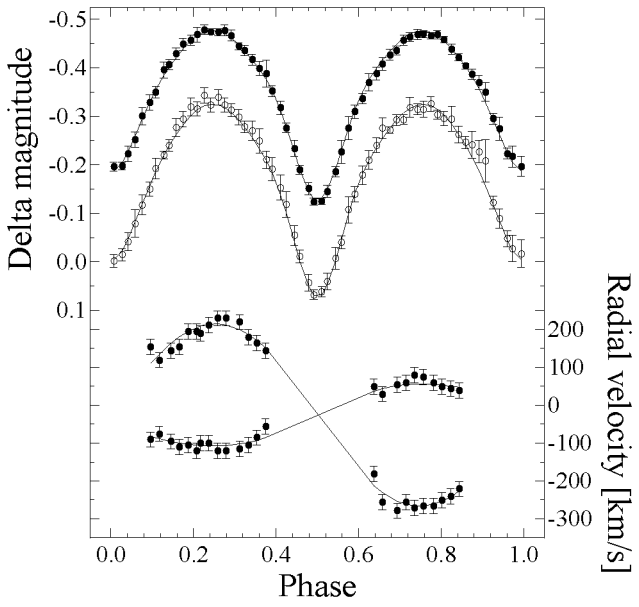

Fig. 3. Result of fitting the Roche-geometry to the 1992 light curve and the radial velocity curve simultaneously. The parameters of the system are collected in Table 2. The fitted curve was used for the spotfitting. Upper panel: open circles = B data, filled circles = V data.

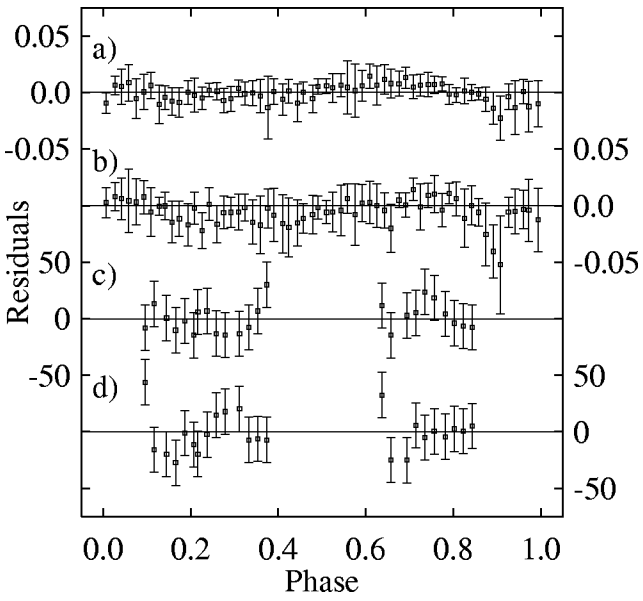

Fig. 4a–d. Residuals of the fit presented in Fig. 3. The labels indicate the following: **a** residual of V light curve (in mag); **b** residual of B light curve (in mag); **c** residual of velocities of the primary (in km s^{-1}); **d** residual of velocities of the secondary (in km s^{-1}).

Table 2. Physical parameters of VW Cephei.

Parameter	Value
q	0.35±0.01
F	1.01±0.01
T [K]	5050 ($fixed$)
i	65.6°±0.3°
$\Delta T/T$	0.078±0.005
v_γ [km s^{-1}]	−16.4±1
a [10^6 km]	1.388±0.01
M_{Total} [M$_\odot$]	1.37

This means that the surface brightness of the primary component is less than that of the secondary. In photometrical point of view it is the same that the hot secondary model assumes. Although the spot model has a more consistent physical basis and it can satisfactorily explain the observations according to Hendry (1997), the hot secondary hypothesis has the advantage that it can reduce the number of adjustable parameters. We have therefore assumed that the light variation during the "quiet activity stage" in 1992 can be described with the hot secondary component. However, it is not yet clear which method produces more reliable geometrical configuration. This interesting problem is being investigated.

The optimization was computed using the Price algorythm described e.g. by Barone et al. (1990). The two (V and B) light curves and the velocity curve were fitted simultaneously. The optimized parameters were the mass ratio (q), the fill-out factor (F, Mochnacki, 1981), the orbital inclination (i), the relative temperature excess of the secondary ($\Delta T/T = X$, as defined in Sect. 1), the gamma-velocity of the system (v_γ) and the semi-major axis of the relative orbit (a). The final set of parameters are collected in Table 2 together with their uncertainties estimated from the spread of the trial points in the parameter space (see Vinkó et al., 1996). The graphical representation of the quality of the fit can be seen in Fig. 3 and Fig. 4.

Comparing our final parameters with those of previous investigators some interesting conclusions can be drawn. First, the gamma-velocity of the system varies considerably due to the orbital motion of the eclipsing pair caused by the third component, VW Cep C. This can be seen easily comparing the gamma-velocity determined by Hill (1989) for the mid 80's (−9 km s^{-1}) with our new value (−16 km s^{-1}). Second, the fill-out factor is very close to 1 indicating a shallow contact. This is in good agreement with earlier results (e.g. Mochnacki, 1981) and justify the validity of the F = 1.0 approximation used by Hill (1989). Third, the newly derived mass ratio is between the earlier published extreme values q = 0.27 (Hill, 1989) and q = 0.41 (Binnendijk, 1967), and it is in good agreement with the recent result of Hendry (1997). It is worth mentioning that within the domain of the earlier published q values the mass ratio is entirely determined by the velocity curve of the primary, which is difficult to measure as it was shown in the previous section. We were able to reproduce the shape of the light curve using the q = 0.41 and q = 0.27 values as fixed parameters with only slight changes of the other variables (similarly to the results of Yamasaki, 1982). This is due to the partial eclipses of VW Cep that was shown to result in large parameter uncertainties when only the light curve is used for the analysis.

As Table 2 indicates, the model produced a relatively high temperature excess of the secondary ($\Delta T/T$ = 0.078) which corresponds to ΔT = 400 K. Equivalently, this may also mean

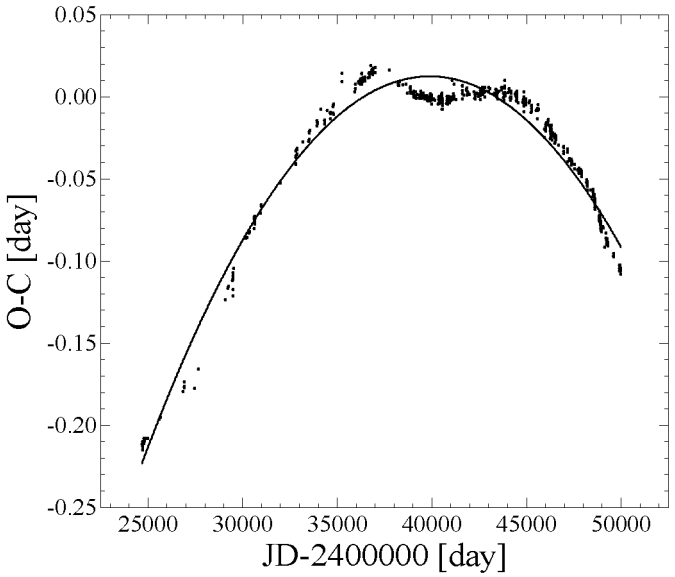

Fig. 5. The $O-C$ diagram of VW Cep based on the ephemeris given in $GCVS$. The fitted parabola gives $\Delta P/P = -0.58{\cdot}10^{-9}$ for the long-term period variation. The effect of the third component star can also be seen as an oscillation around the fitted curve.

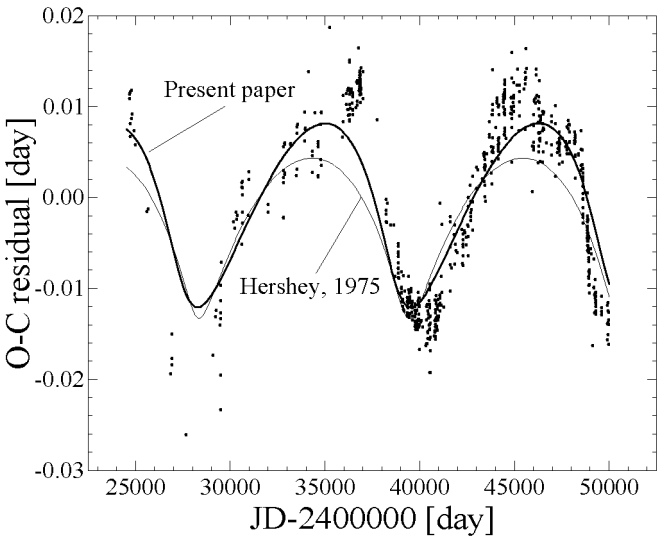

Fig. 6. The $O-C$ diagram with the long-term variation removed. The solid curves are solutions for period variation due to orbital motion of the eclipsing pair VW Cep AB caused by the third star VW Cep C.

that the primary was heavily spotted even in the "quiet" season. Very high resolution spectroscopic observations with very high signal-to-noise ratio might help to distinguish between the two possibilities in the future.

4. Period variation

The period variation of VW Cep was investigated collecting the available times of minima and constructing the $O-C$ diagram (Fig. 5). This diagram is based on mainly photoelectric measurements and some photographic points at the earlier epochs. Most of the data came from the list of Karimie (1983) where the references of the individual minima can be found. The new observations (made after JD 24450000) were collected from recent IBVS volumes and BBSAG, BAA-VSS and BAV publications. The very extensive list of the times of minima together with the accompaining references can be requested from the authors[1] via e-mail.

As it was recognized before, the $O-C$ diagram shows period variations on different timescales. The long-term period change dominates the $O-C$ residuals as a negative parabolic trend. We assumed that it can be described with a parabola indeed (representing a continuous period decrease), and derived the following formula:

$$O-C = a_0 + a_1\ x + a_2\ x^2$$

with $x = JD - 2400000$, $a_0 = -1.666{\pm}0.042$, $a_1 = (8.4{\pm}0.2){\cdot}10^{-5}$, $a_2 = (-1.05{\pm}0.03){\cdot}10^{-9}$.

Previous investigators (Karimie, 1983; Lloyd et al., 1992) preferred discrete period chages at approximately 20 year-long intervals as an explanation of the long-term variation. The available information is not enough to distinguish between the possibilities of continuous or discrete period changes. The broken lines given by the authors mentioned above and the parabolic fit presented here describes the $O-C$ data equally well.

If the continuous period variation is real then the coefficient of the quadratic term corresponds to the rate of the relative period decreasing: $\Delta P/P = 2\ a_2\ P$. Assuming that it is due to conservative mass transfer from the primary (more massive) component to the secondary, the resulting mass transfer rate is $\Delta m = 1.4{\cdot}10^{-7}\ M_\odot$/year. The large rate of either the mass transfer or the period decrease indicate that this phenomenon should be a temporary one as far as the lifetime of the VW Cep system is concerned. The theoretically estimated lifetimes of contact binaries range from $5{\cdot}10^7$ years to $5{\cdot}10^9$ years. Such kind of period variation is predicted by e.g. the Thermal Relaxation Oscillation theory (TRO, Lucy & Wilson, 1979). The following discussion is based on the assumption of continuous period change.

Subtracting the parabolic term from the $O-C$ residuals, the result is plotted in Fig. 6. The cyclic behavior of this diagram was explained as a light time effect (LITE) by several authors (Payne-Gaposchkin, 1941; Schmidt & Schrick, 1955; Hershey, 1975). The computed astrometric orbit (Hershey, 1975; Heintz, 1993) and the visual detection of the 3rd component itself (Heintz, 1975) made the existence of the LITE evident. However, as the data in Fig. 6 show, the LITE curve of Hershey (1975) is inconsistent with the amplitude of the observed residuals.

In order to study this problem, we computed new orbital elements of the VW Cep AB (the eclipsing pair) orbit around the mass center of the triple system. The parameters are listed in Table 3. It can be seen that the new solution fits the observations

[1] K.Szatmary@physx.u-szeged.hu

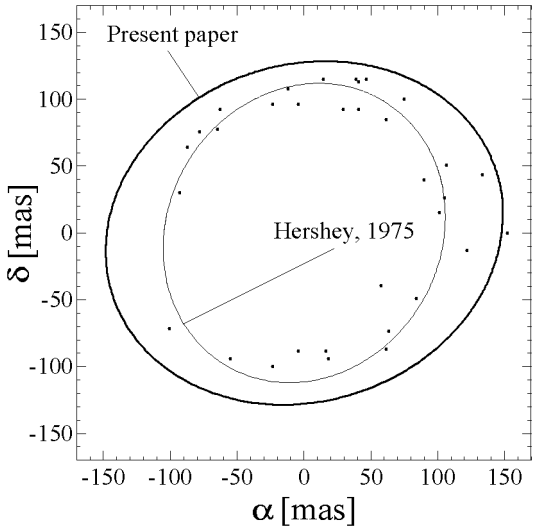

Fig. 7. The computed astrometric orbit using parameters from LITE fitting and Hershey's inclination (Hershey, 1975) (thick line), as well as Hershey's original elements (thin line). This new solution is inconsistent with the astrometric data (dots) which indicates that the third component physically perturbs the period of the eclipsing pair.

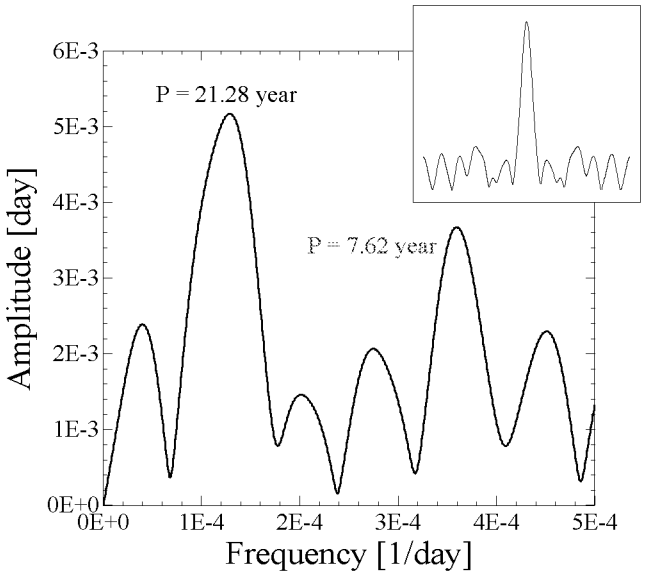

Fig. 8. Fourier spectrum of the $O-C$ data corrected for the long-term variation and the 3rd body orbit derived from Hershey's elements. The peaks appearing at P = 21 year and P = 7.6 year are clearly visible. The spectral window is also shown in the insert.

Table 3. Parameters of the light-time curve. Despite that the new solution fits the $O-C$ data better, the orbital elements in the 3rd column cannot be accepted as the true orbit because of the disagreement with the astrometric data (Fig. 7).

Parameter	Hershey, 1975	Heintz, 1993	this paper
P_{orb} [yr]	30.45±1.17	29	30.89±0.02
i	29.°2	21°±5°	–
a_1 [10^6 km]	474.3±7.3	571.8	–
$a_1\ sin\ i$ [10^6 km]	231.4±3.6	204.9	277±1
e	0.595±0.028	0.65	0.431±0.003
ω	255.°5	87°	221.4°±0.4°
Ω	0.°9	340.°5	–
τ [JD]	2439301±73	2439126	2438651±12
t_0 ($O-C$ = 0) [JD]	–	–	2442829±7
K_1 [km s^{-1}]	1.88±0.15	1.85	1.98±0.01
$f(M_3)$ [10^{-3} M$_\odot$]	4±1	3	6.7±0.1
A_{O-C} [10^{-3} d]	9±1	8	10.13±0.05
d [pc]	24.4±1.2	26.2±1.3	–

better. However, this new orbit is not a physically acceptable one as it is shown Fig. 7 where the astrometric measurements of Hershey (1975) are plotted together with the computed projected orbits (using d = 24.4 pc for the distance of VW Cep). It is clearly visible that the new "orbit" presented here is incompatible with the astrometric data, while that of Hershey (1975) is in good agreement with the observations. The parallactic distance of the VW Cep system given by Hershey (1975) and Heintz (1993) agrees very well (Table 3), so the inconsistency of the new LITE orbit with the data is probably not due to the erroneous distance of VW Cep. Therefore we explain the deviation of the $O-C$ data from Hershey's LITE curve (Fig. 6) as a real cyclic period variation superimposed on the light time effect. Such kind of period variation may be possible, because the 3rd component may perturb the orbital elements of eclipsing pair with a frequency close to that of the long-period orbital revolution (30 years).

This suspicion might be strengthened if we calculate the Fourier spectrum of the $O-C$ residuals corrected for both the long-term variation and the effect of 3rd body using Hershey's elements. The result is plotted in Fig. 8. It can be seen that the data still contain a $1.29{\cdot}10^{-4}$ day^{-1} periodic component which is close to the 3rd body orbital period. Moreover, the peak at $f = 3.59{\cdot}10^{-4}$ day^{-1} may be connected with the activity cycle described in the previous section. As it is known, the magnetic activity can induce period changes due to structural alterations of the active components of an eclipsing binary (Applegate, 1992). This mechanism was also suggested for explaining the period variation of the contact binary AB And by Kalimeris et al. (1994). On the other hand, van't Veer (1991) has found that long term period changes of contact binaries are not related to periodically varying magnetic fields. However, his study was based on a statistical method applied to many systems. Therefore we cannot exclude the presence of this phenomenon in some individual cases.

Both of the effect of the third body and the magnetic activity are also supported by the Fourier spectrum of the Min II−Min I times of minima differences (Fig. 9). The times of minima differences are free from the long-term and 3rd body effects. Removing the P = 63 years term (which origin is uncertain due to the limited length of the data set) two peaks appear at $f = 1.06{\cdot}10^{-4}$ day^{-1} and $f = 2.88{\cdot}10^{-4}$ day^{-1} which are remarkable close to the periods shown in Fig. 8. Note that the times of minima differences were also studied by Hill (1989)

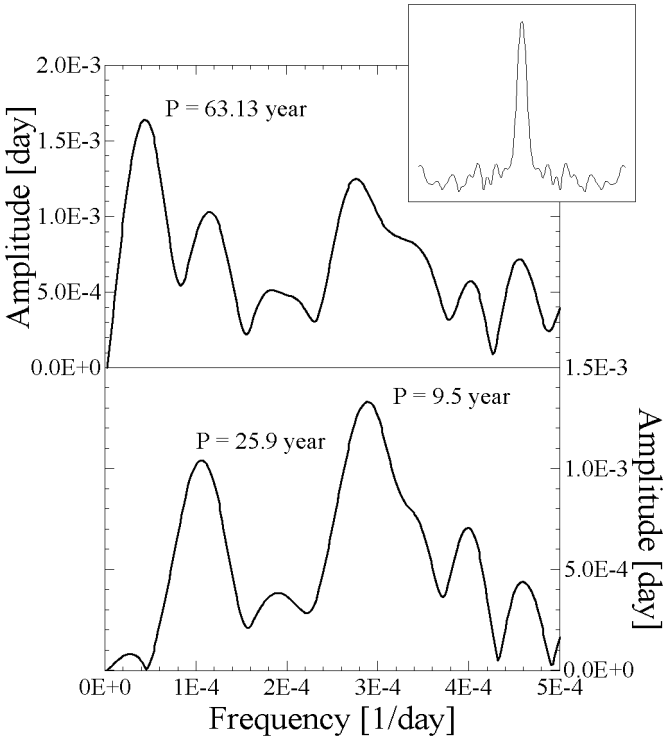

Fig. 9. Fourier spectra of the times of minima differences (Min I−Min II, upper panel). These data are free from the long-term and 3rd body effects. Removing the P = 63 years term (which origin is uncertain due to the limited length of the data series) the peak at P = 9.5 years is apparent (lower panel). This gives further support for the conclusion that the period of the eclipsing pair slightly varies due to structural changes caused by the stellar activity.

pointing out a cycle length of 44 years from less number of data. The two shorter periods mentioned above are well supported by the good-quality photoelectric data obtained in the past 10 years which were obviously not available for Hill.

In summary, we conclude that the period variation of VW Cep can be explained by two additional effects beside the two basic components (long-term change and LITE) known earlier. The first one is due to the tidal perturbation of the 3rd body, while the second one can be attributed to the effect of magnetic activity of VW Cep. Nevertheless, the amplitude of these period changes are close to the detection limit, therefore the existence of these mechanism cannot be undoubtedly proven from the present data. Future observations would help to study the interesting problem of connection between the magnetic activity and period variations.

5. Spot modeling

The observed differences between the 1992 and 1995 seasonal light curves were analyzed by fitting dark spots onto the surface of the primary component. We applied the same method as Yamasaki (1982) and Hendry et al. (1992) adopting a master light curve to take into account the effect of eclipses, geometric distortions and 3rd light. The 1992 seasonal light curve was considered unspotted and it was selected as the master curve. This curve was then removed from the 1995 seasonal data to produce a "spot" light curve. Before this procedure the magnitudes were transformed into intensities.

Table 4. Parameters of spots for 1995.

Parameter	First Spot	Second Spot	Third Spot
λ	$58°\pm10°$	$186°\pm5°$	$292°\pm9°$
ϕ	$27°\pm19°$	$-44°\pm22°$	$68°\pm23°$
r	$11°\pm2°$	$32°\pm4°$	$23°\pm7°$

Table 5. Parameters of spots for 1992.

Parameter	First Spot	Second Spot
λ	$50°\pm8°$	$236°\pm4°$
ϕ	$37°\pm16°$	$32°\pm16°$
r	$6°\pm3°$	$7°\pm4°$

The "spot" light curve was then investigated with the modified version of the program *SPOT* developed by E.Budding. This code fits circular spots with fixed flux ratio $F_{spot}/F_{photosphere}$ onto a surface of a spherical star taking into account the effect of limb darkening. Because the difference curve does not contain the variation due to eclipses, geometric distortions and 3rd light, the assumption of the sphericity of the spotted component caused only negligible error in the spot solution.

Only the primary, more massive component was assumed to be spotted, similarly to Hendry et al. (1992). This assumption was also supported by the $H\alpha$ emission excess of that component (see Sect. 6). The remaining (constant) intensity of the secondary component was taken into account with an intensity ratio $I_1/(I_1 + I_2)$ = 0.71 both in V and B bandpasses. The spot temperatures were assumed to be 4000 K which resulted in assuming almost completely dark spots. This large temperature difference between the photosphere and the spot area may be supported by the absence of noticeable color variation due to the spots (the color curves of the 1992 and 1995 season are very similar while the V light curves are markedly different, see Fig. 1). On the other hand, the accuracy of our color curves did not allow us to determine the spot temperature as a free parameter.

The resulting spot coordinates for the 1995 season are collected in Table 4. The uncertainties are formal errors of the least-squares fitting estimated from the curvature of the Hessian matrix. The graphical representation of the derived spot configuration is presented in Fig. 10. This configuration is very similar to the one computed by Hendry et al. (1992). Three spots (or spot groups) are necessary to model the light curve variation. The largest spot is located on the "southern" hemisphere at the back of the primary. The only exception is that in our solution the "throat" region is not as heavily spotted as it is in Hendry et al. (1992, see their Fig. 7). The synthesized spot light curves in B and V are plotted in Fig. 11.

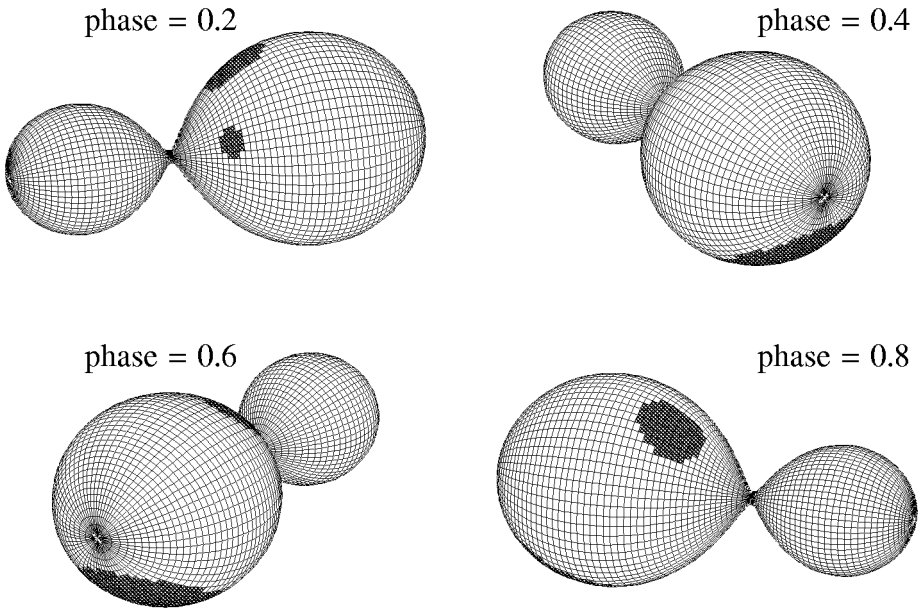

Fig. 10. Spot distribution on the surface of VW Cep in 1995. In order to minimize the number of free parameters circular spots were assumed on the surface of the primary component only.

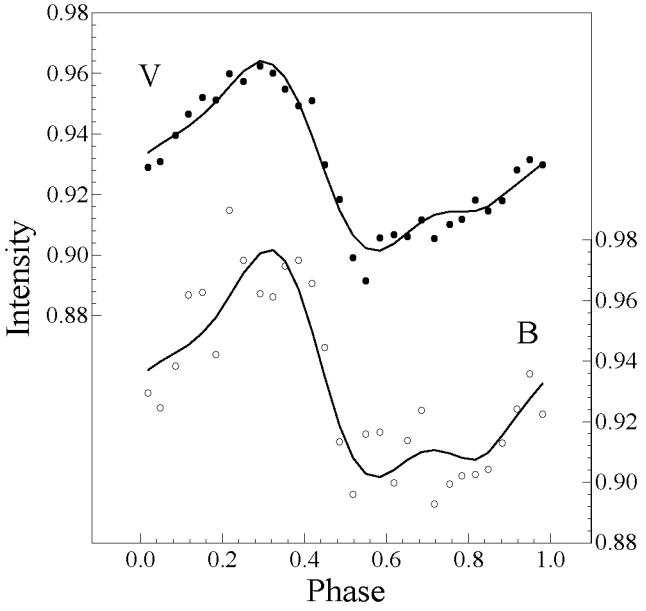

Fig. 11. Observed (circles) and modeled (lines) "spot" light curves in V and B for the 1995 data. The data points were computed by removing the effect of eclipses, geometric distortions and the third light from the observed light curves. The synthetic lines were generated by fitting circular spots on a spherical surface. The light curve disturbances can be explained with three independent dark spots (or spot groups) distributed on the surface of the primary.

In order to test the minimum recoverable spot size, the 1992 light curves were also analyzed with the spotfitting code in a similar way. Because these light curves were assumed unspotted, they contain mostly observational noise. The fitting resulted in two spots listed in Table 5 located on the two sides of the larger component. The recovered spot radii are $6° - 7°$. Since the resulted spot radii for the 1995 season are larger by at least a factor of 2, the "1995 spots" can be considered significant and probably not due to random noise.

Table 6. Spot coverage of primary component.

Year	No. of Spots	Coverage (%)
1987	2	2.0
1992	2	0.6
1995	3	12.5

Table 6 lists the spot coverage of the primary component (spotted area / total area of the surface $\times$ 100) determined from the seasonal light curves. It can be seen that in the case of increased activity the spottedness of the surface can be 20 times larger than during the lower activity stage. Note, however, that the assumption of the hot secondary reduces the spot coverage of the primary, which means that this parameter can be even larger if the spots are fully responsible for the W-type light curve of VW Cephei.

6. Line profile analysis

With the help of the new physical parameters determined in Sect. 3, it is possible to compute the line profiles of the system in order to study the two components separately and look for additional phenomena related to surface activity. For this purpose, we applied the method of spectrum synthesis to our telluric-corrected, time-resolved optical spectra (Sect. 2.2). This method uses the theoretical Doppler-broadening function of the system and a reference spectrum of either a slowly rotating star with similar spectral type as that of the binary, or a model atmosphere in order to synthesize the line profiles of the contact system. Because the components of the contact binary have almost the same effective temperature and very similar surface gravity, one reference spectrum is sufficient to represent the

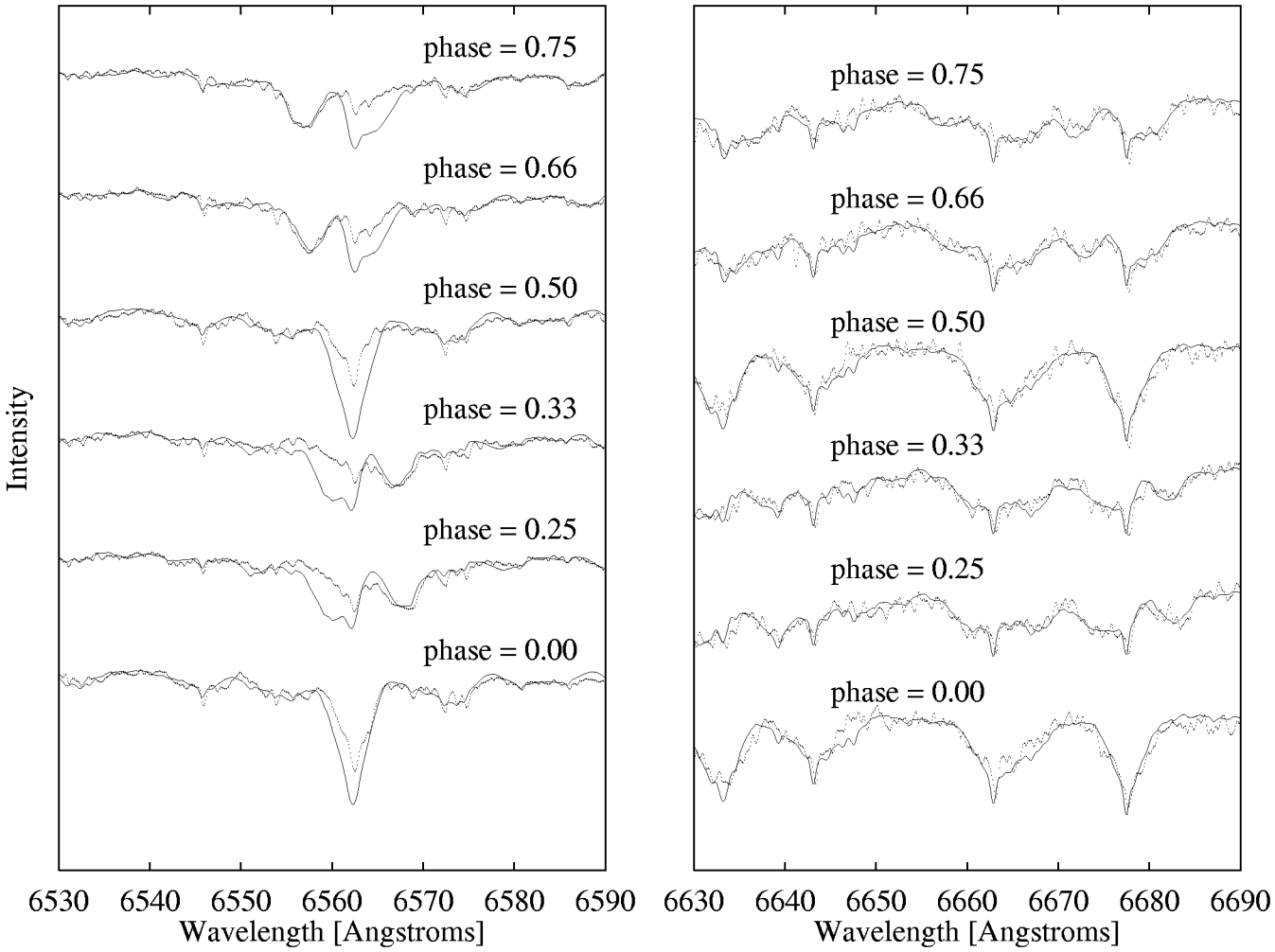

Fig. 12. The model computation of the optical spectra (continuous curve) compared with the observations (dotted curve) at different orbital phases. The line profile changes due to the orbital revolution is clearly seen. The $H\alpha$ profile (left panel) shows the lack of absorption of the primary component. This can be interpreted as a chromospheric emission (due to stellar activity) that fills the absorption core. This gives an evidence that the activity is driven by the larger, more massive star. However, the synthetic and observed curves are in good agreement in case of metallic lines (right panel).

shape of the lines of the system. The reference stars were the same velocity standards as mentioned in Sect. 2.2.

The broadening profiles were computed using a newly developed program *WGMODEL*. This code works with large number of triangular surface elements projected onto the Roche-surface (similarly to *GDDSYN*, Hendry & Mochnacki, 1992). It also takes into account limb- and gravity-darkening, reflection (using a simple spherical approximation), hot secondary and dark spots on the surface of the primary. The number of surface elements can be arbitrarily large, so the output profile can be synthesized with very high resolution.

The computed broadening profiles were tested with the *WUMA4* code (Rucinski, 1974), and reasonable agreement has been found. The new geometrical and physical parameters collected in Table 2 were used throughout the spectral synthesis.

The final synthesized spectra were derived as a convolution of the reference spectrum with the broadening profiles corresponding to the observed orbital phases of VW Cep. The effect of the third component was estimated by adding 10 percent of the reference spectrum to the convolved one and re-normalizing it to the continuum. It means that we neglected the difference between the spectral type of the contact binary and the third component. However, this probably does not cause any significant error in the line profile synthesis, because of the faintness of the third companion and the lower signal-to-noise of our spectra.

The synthesized spectra can be compared with the observed spectra of VW Cep as they are plotted in Fig. 12. The Doppler-shift between the reference spectrum and that of VW Cep was taken into account using the velocities in Table 1. Slight wavelength-dependent errors in the continuum-normalization of the VW Cep spectra were corrected by fitting a second-order polynomial to the region outside $H\alpha$ and subtracting this fitted curve from the original spectra. It turned out that using HD 212943 ($K0$) as a reference star, the synthesized spectrum

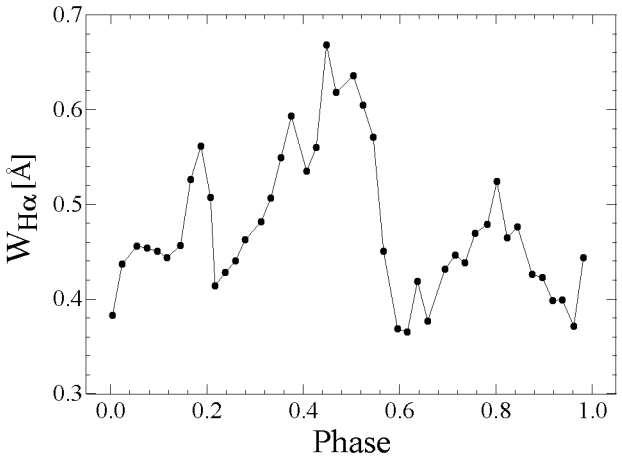

Fig. 13. The intensity of the chromospheric emission as a function of phase. The strongest emission occurs when the primary is in front.

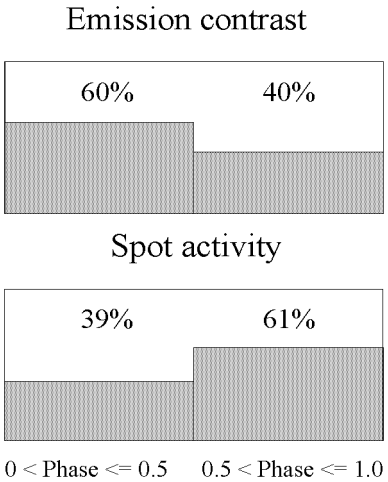

Fig. 14. Block diagrams showing emission contrast (upper panel) and spot activity (lower panel) as a function of orbital phase. The strength of emission shows an anti-correlation with the spottedness of the surface.

shows better agreement with the spectrum of of VW Cep than using HD 204867 ($G0$). This agrees well with the spectral type $G8 - K0$ found by Popper (1948), but it also means that the $G5$ spectral type sometimes quoted in the literature (e.g. Barden, 1985) is inapplicable. As the referee pointed out, the mean $B-V$ color of VW Cep (0.86) also indicates later spectral type.

The $H\alpha$ line strength of the secondary component (Fig. 12, left panel) could be reproduced only with the hot secondary hypothesis (we adopted $\Delta T/T$ = 0.079 from Table 2), but without any spots. An attempt was made to detect any effect of spots on the metallic lines (right panel), however, the S/N ratio was not high enough to enable that.

The $H\alpha$ line of the primary component shows a definite lack of absorption which can be interpreted as a chromospheric emission filling the line core. This phenomenon was detected in other W UMa-stars (Barden, 1985, 1987) and more recently in VW Cep itself (Frasca et al., 1996). We investigated the phase dependence of the emission by subtracting the synthesized spectra from the observed ones and determining the equivalent width (EW) of the emission component. The EW was calculated in a 10 Å wide window around the central wavelength of the primary star. The emission EW as a function of phase is plotted in Fig. 13. Note, that the maximum value is less than that observed by Frasca et al. (1996) by 0.3 Å, which is probably due to the difficulties of the continuum-normalization around $H\alpha$. For example, a 0.03 error in the level of the continuum produces a 0.3 Å error of the EW values which can explain this disagreement. The amplitude of the curve in Fig. 13 is consistent with that presented by Frasca et al. (1996).

It is visible that the strongest emission occurs during the occultation eclipse, i.e. when the primary is in front (the phases are similar to those defined in Sect. 2.1). It fully confirms the conclusions of previous observations (Barden, 1985) as well as theoretical expectations (Rucinski, 1992, 1994) that the primary, more massive component has thicker convective zone and, hence, it shows increased activity.

In order to enhance the emission contrast between the two opposite sides of the components, an offset value of 0.35 Å was subtracted from the curve in Fig. 13. This curve was then integrated between 0.0 and 0.5 phases (I_1), and between 0.5 and 1.0 phases (I_2). The relative quantities $I_i/(I_1 + I_2)$ for $i = 1, 2$ are plotted as a block diagram in Fig. 14 (upper panel). A similar parameter was defined to measure the spot activity of the system using the spot light curve in V presented in Fig. 11. The intensity values were subtracted from 1.0 and integrated in a similar way as above (lower panel in Fig. 14). It can be seen that the emission is slightly larger between 0.0 and 0.5 phases than in the $0.5 - 1.0$ phase interval, while the opposite effect can be observed for the spot activity. It means that the chromospheric emission dominates on the less spotted hemisphere of the primary, therefore the emission intensity is slightly anti-correlated with the spot coverage. Such anti-correlation was found e.g. in the case of AB Dor (Cutispoto & Pallavicini, 1992).

Frasca et al. (1996) also reported the lack of enhanced $H\alpha$ emission during eclipses. Their observations were made in 1993 when VW Cep showed less activity compared to the 1995 season (based on the shape of the light curve). The fact that our Fig. 13 clearly shows increased emission in the transit eclipse may indicate that the chromospheric emission of the primary component is stronger when the system is more active.

However, we did not find any evidence for the P Cygni-profiles observed by Frasca et al. (1996). Since our reciprocal dispersion (10 Å/mm) is lower than that of Fasca et al. (40 Å/mm), we think that this phenomenon is either an instrumental artifact or a temporary effect. Therefore, we believe that the explanation using gaseous streams in a semi-detached configuration proposed by Frasca et al. (1996) is unlikely for VW Cep. Both our photometric and spectroscopic modeling resulted in a consistent picture of VW Cep being in marginal contact (F = 1.01). As it was pointed out in many earlier papers, the contact state is necessary for W UMa-stars in order to ex-

plain the luminosity and temperature excess of the less massive, secondary component.

7. Conclusions

Based on the results presented in the previous sections we draw the following conclusions:

1. The existence of an at least 7 year-long activity cycle of VW Cep was confirmed based on new multi-color photometry.

2. New physical parameters of the system were computed using the probably unspotted light curves and a new cross-correlation velocity curve. It was shown that the mass ratio is between the two extreme values published previously for this system.

3. Assuming a continuous long-term period variation and using Hershey's elements for the 3rd body, the corrected $O-C$ residuals still contain at least two cyclic components. One of them may be due to real period variation caused by the perturbation of the 3rd companion. The other one has a cycle length close to $7-8$ years indicating that the surface activity might be responsible for that. These are also supported by the behavior of the times of minima (Min I−Min II) differences.

4. The light curve perturbations observed in 1995 were modeled by dark starspots. The spot coverage of the primary was at least 12 per cent in that season.

5. $H\alpha$ emission of the primary component was observed spectroscopically in the same season, while such kind of emission was not detected on the secondary. This fact supports the hypothesis that the primary, more massive component drives the activity of the system. A possible anti-correlation between the $H\alpha$ emission and spot visibility was pointed out. No P Cygni-profiles reported by Frasca et al. (1996) were observed in the $H\alpha$ region of VW Cep.

Acknowledgements. Most of this work was made during the visits of J.V. and J.G. to the Department of Astronomy University of Toronto and David Dunlap Observatory, Richmond Hill, Canada. The authors are grateful to Profs. J.R. Percy, J.D. Fernie and N.R. Evans for their generous support. Thanks are also due to Prof. E. Seaquest (Director), Dr. K.Kamper and J.Thomson for kindly granting telescope time at DDO and assisting during the spectroscopic observations. Fruitful discussions with Prof. S.M. Rucinski, Prof. S.W. Mochnacki and P.D. Hendry are gratefully acknowledged. The authors also express their thanks to the staff of Konkoly Observatory for the accessibility of the observing facilities. This work was funded partly by Hungarian OTKA Grants No. F022249, T022259, W015239, the Eötvös Fellowship of J.V., the Soros Foundation Travel Grant No. 222/2/3624 of G.K., the doctoral fellowship of J.G. and the student fellowships of G.K., L.L.K. and T.B..

References

Applegate, J.H., 1992, ApJ 385, 621
Barden, S.C., 1985, ApJ 295, 162
Barden, S.C., 1987, ApJ 317, 333
Barone, F., Milano, L., Russo, G., 1990, in: "Active Close Binaries" (ed: C. Ibanoglu), p. 161
Binnendijk, L., 1967, Publ. Dom. Astrophys. Obs. 13, 27
Binnendijk, L., 1970, Vistas Astron. 12, 217
Bradstreet, D.H., Guinan, E.F., 1988, in: "A Decade of UV Astronomy with IUE", ESA SP-281, Vol.1, p. 303
Cutispoto, G., Pallavicini, R., 1992, in: "Surface Inhomogeneities on Late-Type Stars", Lecture Notes in Physics No. 397 (ed. P. B. Byrne, D. J. Mullan) Springer-Verlag, p. 264
Eaton, J.A., Wu, C.-C., Rucinski, S.M., 1980, ApJ 239, 919
Eggen, O.C., 1967, Mem. Roy. Astron. Soc. 70, 111
Frasca, A., Sanfilippo, D., Catalano, S., 1996, A&A 313, 532
Heintz, W.D., 1975, ApJS 29, 315
Heintz, W.D., 1993, PASP 105, 586
Hendry, P.D., Mochnacki, S.W., 1992, ApJ 388, 603
Hendry, P.D., Mochnacki, S.W., Collier Cameron, A., 1992, ApJ 399, 246
Hendry, P.D., 1997, PhD thesis, University of Toronto
Hershey, J.L., 1975, AJ 80, 662
Hill, G., 1989, A&A 218, 141
Kalimeris, A., Rovithis-Livaniou, H., Rovithis, P., Oprescu, G., Dumitrescu, A., Suran, M.D., 1994, A&A 291, 765
Karimie, M.T., 1983, Ap&SS 92, 58
Kiss, L.L., Gál, J., Kaszás, G., 1995, IBVS No. 4181
Kreiner, J.M., Winiarski, M., 1981, Acta Astron. 31, 351
Kuiper, A., 1941, ApJ 93, 133
Kwee, K.K., 1966a, BAIN Suppl. 1, 245
Kwee, K.K., 1966b, BAIN Suppl. 1, 265
Kwee, K.K., 1966c, BAIN 18, 448
Linnell, A.P., 1986, ApJ 300, 304
Linnell, A.P., 1991, ApJ 383, 330
Lloyd, C., Watson, J., Pickard, R.D., 1992, IBVS No. 3704
Lucy, L.B., 1968, ApJ 151, 1123
Lucy, L.B., Wilson, R.E., 1979, ApJ 231, 502
Mochnacki, S.W., 1981, ApJ 245, 650
Mullan, D.J., 1975, ApJ 198, 563
Payne-Gaposchkin, C., 1941, Publ. Am. Astron. Soc. 10, 127
Popper, D.M., 1948, ApJ 108, 490
Pustylnik, I., Sorgsepp, L., 1976, Acta Astron. 26, 319
Rucinski, S.M., 1974, Acta Astron. 24, 119
Rucinski, S.M., Seaquist, E.R., 1988, AJ 95, 1837
Rucinski, S.M., 1992, AJ 103, 960
Rucinski, S.M., 1993, in: "The Realm of Interacting Binaries" (ed: J.Sahade et al.) Kluwer Acad.Publ., p. 111
Rucinski, S.M., 1994, AJ 107, 738
Schilt, J., 1926, ApJ 64, 221
Schmidt, H., Schrick, K.W., 1955, Z. Astrophys. 37, 73
Stepien, K., 1995, MNRAS 274, 1019
Tsuru, T., Makishima, K., Ohashi, T., Sakao, T., Pye, J.P., Williams, O.R., Barstow, M.A., Takano, S., 1992, MNRAS 255, 192
van't Veer, F., 1973, A&A 26, 357
van't Veer, F., 1991, A&A 250, 84
Vilhu, O., Walter, F.M., 1987, ApJ 321, 958
Vilhu, O., Caillault, J.-P., Heise, J., 1988, ApJ 330, 922
Vinkó, J., 1989, IBVS No. 3291
Vinkó, J., Gál, J., Szatmáry, K., Kiss, L.L., 1993, IBVS No. 3965
Vinkó, J., Hegedüs, T., Hendry, P.D., 1996, MNRAS 280, 489
Walter, K., 1979, A&A 80, 27
Wilson, R.E., Devinney, E.J., 1971, ApJ 166, 605
Wilson, R.R., 1979, ApJ 234, 1054
Yamasaki, A., 1982, Ap&SS 85, 43

This article was processed by the author using Springer-Verlag LaTeX A&A style file *L-AA* version 3.